DASSAULT SYSTEMES

BIOVIA

HIGH-THROUGHPUT INVESTIGATION OF PAH

APPLICATION BRIEF

This application demonstrates the use of dispersion corrected DFT code in CASTEP in establishing a basis for high-throughput screening of molecular crystalline materials, enabling associating crystal/electronic structure with important properties such as band gap of a material.[1]

INTRODUCTION

The quest for inexpensive, flexible, lightweight materials for use in electronic applications has led researchers to explore what useful arrays can be constructed through organic means, and the ability to predict useful properties within organic-electronic materials is quickly becoming an essential part of organo-electronic product design. Polycyclic aromatic hydrocarbons (PAH) make up a group of organic molecular crystals (OMC) which have shown promise for use in electronics and electro-optics[2,3]. Despite their versatility and abundance, theoretical exploration of the electronic properties of most crystalline PAHs remains uncharted. It is demonstrated here that one can use dispersion inclusive density functional theory (DFT) to shed light onto the structural and electronic trends occurring within this promising group of materials.

Traditionally, PAHs can be either heterocyclic or only carbon containing, and assemble in molecular crystalline arrays under ambient conditions. Those PAHs containing only hydrogen and aromatic carbon can be classified into five crystalline motifs, definable by the π^o-parameter (a product of the inter-planar angle between molecular components and the fraction of C•••C intermolecular close contacts[4]). The five motifs: a) herringbone (HB) b) sandwich-herringbone (SHB) c) beta-herringbone (β-HB) d) gamma (γ) and e) beta (β) are depicted in Figures 1a-1e using structures which exemplify the characteristics of each motif [5,6].

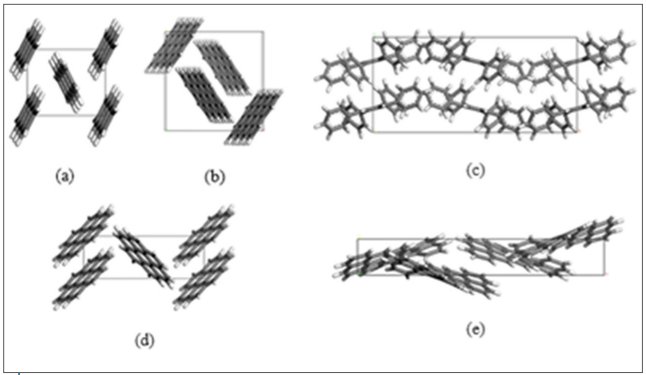

Figure 1. PAH motifs. a) HB - anthracene [ANTCEN]. b) SHB – Quaterylene [QUATER10]. c) β-HB – 1, 2, 3, 4, tetraphenylbenzene [FOVVOB]. d) γ – coronene [CORONE01]. e) β – anthra[2,1,9,8-hjkl]benzo[de]naphtha [2,1,8,7-stuv]pentacene [BOXGAW].

Despite the extensive knowledge of gas phase PAH band gap trends, little is known about the band gap vs. structural/motif dependence in crystalline PAHs. Dispersion inclusive density functional theory had been used previously to investigate the oligoacenes[7,8] (a prototypical group of PAHs) in great detail. In those studies (as well as others[9,10]), the Tkatchenko-Scheffler dispersion energy method (PBE+vdW) had been benchmarked for structural and properties predictions of molecular crystals with a specific aim on the larger PAH family. The oligoacene investigations mentioned above demonstrated that PBE+vdW can provide excellent structural agreement with experiment, as well as accurately model the pressure-induced structural changes of naphthalene, anthracene, and pentacene. PBE+vdW was also used to reproduce the pressure-induced phase transition of tetracene along with the pressure-induced changes to the HOMO-LUMO band gaps of tetracene and pentacene. With the aforementioned success, the stage had been set for investigating the structural and electronic trends of all 91 PAHs currently in the Cambridge Structural Database (CSD) in order to gain further chemical insight into this unique class of crystals.

By estimating the Bond Dissociation Energy (BDE) leading to the formation of the radical(s), the energetic balance can be obtained. Such BDEs can be measured experimentally and have also been the subject of recent computational studies[2]. It is assumed that the propensity toward autoxidation is characterized by the bonding strength of the weakest hydrogen.

The aim of the present study was therefore (i) to estimate, using DFT-based calculations, the BDEs of X-H bonds (X = C, N, O, S) and, for a reference subset of 45 compounds, to validate the computational settings against known published data and (ii) to validate against a known subset of APIs. Following this validation process, the methodology can be used for early compound stability profiling.

METHODOLOGY

All PAH structures investigated were acquired as referenced in the CSD (reference codes have been provided). All selected PAH structures contain only hydrogen and aromatic carbon atoms.

Density functional theory with dispersion interactions as implemented in the CASTEP program was used for the optimization of the PAH crystal structures using the Perdew-Burke-Ernzerhof exchange-correlation functional (PBE)[11] with the Tkatchenko-Scheffler dispersion energy method (+vdW)[12]. Isolated molecular band gaps (E_g^{Mol}) were also calculated in CASTEP using the same convergence criteria as used for the crystals except the E_g^{Mol} being calculated on the optimized molecules using only Gamma point. Molecules were placed in a periodic cell with a minimum of 10 Å to the cell boundary before geometry optimization.

Band gaps were obtained without dispersion correction as the fully self-consistent implementation of the PBE+vdW method leads to negligible modifications of electronic properties for molecular crystals. The long-range van der Waals energy was determined from the TS-method; i.e., the difference between the PBE total energy and the dispersion-corrected total energy. The entire set of calculations and corresponding analyses was automated through PERL scripting. Problem structures (outliers) were addressed separately and recalculated

RESULTS

The first step in establishing a computational method for use in a high-throughput scenario is to establish its reliability for calculating the structural properties[13,14]. Good agreement between the experimental and calculated crystal structures is demonstrated in Figure 2.

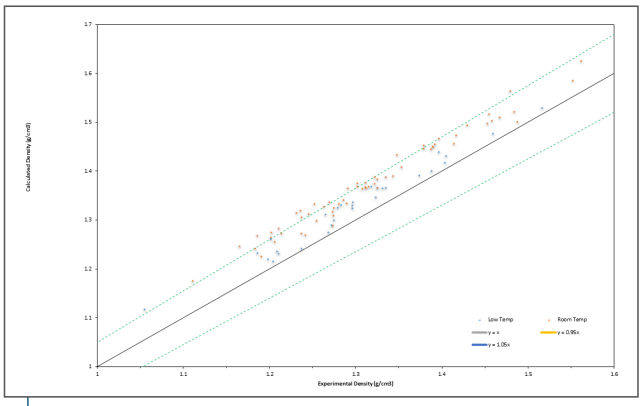

Figure 2: Comparison of calculated and experimental densities for 91 PAHs. Black line represents exact agreement between experiment and calculation. Green dotted lines represent ±5% variation. Red balls are structures obtained at room temperature and blue balls are structures obtained below room temperature.

Figures 3 & 4 show that Kohn-Sham gap (E_g^{KS}) — calculated using PBE (E_g^{PBE}) — does an excellent job of predicting the relative optical gaps of PAHs in both the gas and crystalline phases. Interestingly, it appears that for PAHs, an accurate value of the experimental optical gaps (E_g^{opt}) may be obtained by simply adding a constant of ~ 1 eV (here on called, ξPBE) to E_g^{PBE} regardless of phase. Specifically, ξPBE is 0.99eV for solution/gas phase comparison while ξPBE is 1.05eV for the crystalline phase. The addition of ξPBE results in calculated gaps that differ from E_g^{opt} by only ±2.6% on average for the isolated molecules and ±3.5% on average for the crystalline ensembles. The single parameter fit to the PBE gap is a welcomed finding as E_g calculations utilizing PBE are an order of magnitude cheaper compared to E_g calculations using

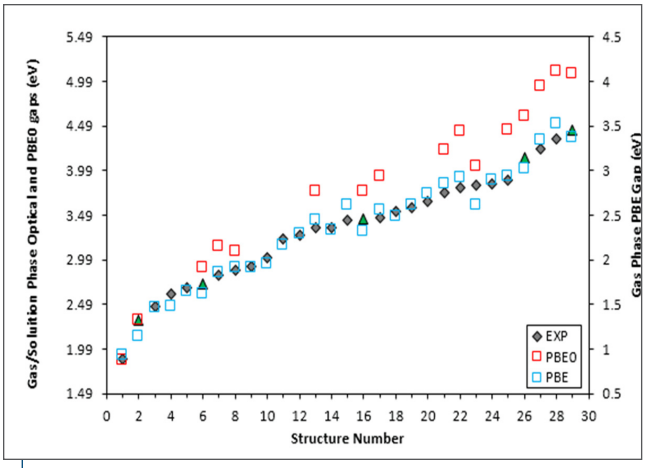

Figure 3: Comparison of predicted and experimental gas/solution phase optical band gaps for select PAHs. E_g^{PBE} are plotted on the secondary vertical axis (on the right), and aligned with experimental values (see details in the text) by shifting the zero crossing of the secondary vertical axis by 0.99 eV relative to that of the primary axis (same scale as the primary axis).

more "precise" methods such as hybrid functionals like PBE0[8], HSE03[8], and B3LYP[15] or quasiparticle corrections[16] and time-dependent methods[15].

DISCUSSION

As revealed in Figure 2, nearly all of the geometry optimized structures (run at 0 K) are denser than experiment. One reason for the difference is that most of the PAH x-ray studies were conducted at room temperature, leading to lower densities than those calculated at 0 K. Despite the temperature difference between calculation and experiment, ~77% of the calculated densities are within +5% of experiment (indicated by green lines in Figure 2). When the x-ray structures were determined at lower temperatures (< 273 K), variation decreases to within +2.3% on average. Some calculated structures corresponding to room temperature X-ray structures were more than +5% as dense; however, no obvious phase/motif transitions were observed via analysis of the space group.

It had been known that E_g^{KS} should not be used to predict fundamental band gaps (E_g^{fun}) of crystalline materials. In the meantime, it had also been shown that E_g^{KS} could correctly predict the trend of decreasing E_g with increasing number of rings in crystalline oligoacenes, from naphthalene (2A) to pentacene (5A)[8]. For molecules in the gas phase, E_g^{KS} had been shown to reliably predict experimental optical gaps (E_g^{opt}) of the PAHs. It is expected that in molecular solids bound by weak intermolecular interactions (such as PAHs) E_g^{KS} could predict E_g^{opt} as in the "normal" molecular situation because strongly bound Frenkel excitons remain localized within the excited molecule[13].

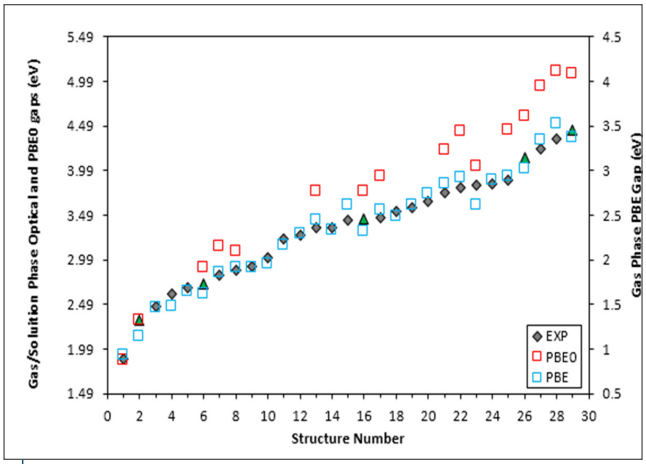

Figure 4: Comparison of predicted and experimental optical gaps of crystalline PAHs. PBE gaps are plotted on the secondary vertical axis (on the right), and aligned with experimental values by shifting the zero crossing of the secondary vertical axis by 1.05 eV relative to that of the primary axis (same scale as the primary axis).

CONCLUSIONS

ADispersion inclusive DFT was shown to capture well the structural and electronic properties of all PAHs available in the CSD. It was found that addition of a ~ 1 eV constant to the DFT-PBE gap provided good agreement with experimental optical gaps. The work established a foundation for an efficient, density functional theory (DFT)-based screening of molecular crystalline materials with respect to structural and electronic properties.

REFERENCES

1. Schatschneider, B., Monaco, S. Liang, J-j., and Tkatchenko, A. High-Throughput Investigation of the Geometry and Electronic Structures of Gas-Phase and Crystalline Polycyclic Aromatic Hydrocarbons. *J. Phys. Chem.* C, **2014**, 118 , 19964–19974

2. Anthony, J. E. The Larger Acenes: Versatile Organic Semiconductors. *Ang. Chem. Int. Ed.* **2008**, 47, 452-483.

3. Sun, Z.; Ye, Q.; Chi, C.; Wu, J. Low Band gap Polycyclic Hydrocarbons: from Closed-Shell Near Infrared Dyes and Semiconductors to Open-Shell Radicals. *Chem. Soc. Rev.* **2012**, 41, 7857 -7889.

4. Schatschneider, B.; Phelps, J.; Jezowski, S. A New Parameter for Classification of Polycyclic Aromatic Hydrocarbon Crystalline Motifs: A Hirshfeld Surface Investigation. *CrystEngComm* **2011**, 13, 7216-7223.

5. Desiraju, G. R.; Gavezzotti, A. From Molecular to Crystal Structure; Polynuclear Aromatic Hydrocarbons. *J. Chem. Soc., Chem. Commun.*, **1989**, 621-623.

6. Desiraju, G. R.; Gavezzotti, A. Crystal Structures of Polynuclear Aromatic Hydrocarbons. Classification, Rationalization and Prediction from Molecular Structure. *Acta Crystallogr. Sect. B Struct. Sci.* **1989**, 45, 473–482.

7. Schatschneider, B.; Monaco, S.; Tkatchenko, A.; Liang, J.-J. Understanding the Structure and Electronic Properties of Molecular Crystals under Pressure: Application of Dispersion Corrected DFT to Oligoacenes. *J. Phys. Chem. A* **2013**, 117, 8323–8331.

8. Schatschneider, B.; Liang, J.-J.; Reilly, A.; Marom, N.; Zhang, G.-X.; Tkatchenko, A. Electrodynamic Response and Stability of Molecular Crystals. *Phys. Rev. B* **2013**, 87, 060104.

9. Schatschneider, B.; Liang, J. J. Simulated Pressure Response of Crystalline Indole. *J. Chem. Phys.* **2011**, 135, 164508.

10. Schatschneider, B.; Liang, J.-J.; Jezowski, S.; Tkatchenko, A. Phase Transition between Cubic and Monoclinic Polymorphs of the Tetracyanoethylene Crystal: The Role of Temperature and Kinetics. *CrystEngComm* **2012**, 14, 4656-4663.

11. Perdew, J.P.; Burke, K.; Ernzerhof, M. Generalized Gradient Approximation Made Simple. *Phys. Rev. Lett.*, **1996**, 77, 3865-3868.

12. Tkatchenko, A.; Scheffler, M. Accurate Molecular Van Der Waals Interactions from Ground-State Electron Density and Free-Atom Reference Data. *Phys. Rev. Lett.* **2009**, 102, 073005.

13. Jain, A.; Hautier, G.; Ong, S. P.; Moore, C. J.; Fischer, C. C.; Persson, K. A.; Ceder, G. Formation Enthalpies by Mixing GGA and GGA + U Calculations. *Phys. Rev. B* **2011**, 84, 045115.

14. Jain, A.; Hautier, G.; Moore, C.J.; Ong, S.P.; Fischer, C.C.; Mueller, T.; Persson, K.A.; Ceder, G. A High-Throughput Infrastructure for Density Functional Theory Calculations. *Comp. Mat. Sci.* **2011**, 50, 2295-2310.

15. Malloci, G.; Cappellini, G.; Mulas, G.; Mattoni, A. Electronic and Optical Properties of Families of Polycyclic Aromatic Hydrocarbons: A Systematic (Time-Dependent) Density Functional Theory Study. *Chem. Phys.* **2011**, 384, 19–27.

16. Sharifzadeh, S.; Biller, A.; Kronik, L.; Neaton, J. B. Quasiparticle and Optical Spectroscopy of the Organic Semiconductors Pentacene and PTCDA from First Principles. *Phys. Rev. B* **2012**, 85, 125307..

17. Baerends, E. J.; Gritsenko, O. V; van Meer, R. The Kohn-Sham Gap, the Fundamental Gap and the Optical Gap: The Physical Meaning of Occupied and Virtual Kohn-Sham Orbital Energies. *Phys. Chem.* **2013**, 15, 16408–16425.

DASSAULT SYSTEMES | The **3D**EXPERIENCE® Company

Dassault Systèmes Corporate
Dassault Systèmes
175 Wyman Street
Waltham, Massachusetts
02451-1223
USA

BIOVIA Corporate Americas
BIOVIA
5005 Wateridge Vista Drive
San Diego, CA 92121
USA

BIOVIA Corporate Europe
BIOVIA
334 Cambridge Science Park,
Cambridge CB4 0WN
England